Voltage-gated K+ channel blocker quinidine inhibits proliferation and induces apoptosis by regulating expression of microRNAs in human glioma U87-MG cells

QIN RU[1,2], XIANG TIAN[1,2], MING-SHAN PI[1], LIN CHEN[1,2], KAI YUE[1,2],
QI XIONG[1,2], BAO-MIAO MA[1,2] and CHAO-YING LI[1,2]

[1]Wuhan Institutes of Biomedical Sciences, Jianghan University, Wuhan, Hubei 430056; [2]Hanjea Institutes of Biomedical Sciences, Hanjea (Wuhan) Biological Technology Co., Ltd., Wuhan, Hubei 430075, P.R. China

Abstract. Accumulating evidence has proved that potassium channels (K+ channels) are involved in regulating cell proliferation, cell cycle progression and apoptosis of tumor cells. However, the precise cellular mechanisms are still unknown. In the present study, we investigated the effect and mechanisms of quinidine, a commonly used voltage-gated K+ channel blocker, on cell proliferation and apoptosis of human glioma U87-MG cells. We found that quinidine significantly inhibited the proliferation of U87-MG cells and induced apoptosis in a dose-dependent manner. The results of caspase colorimetric assay showed that the mitochondrial pathway was the main mode involved in the quinidine-induced apoptotic process. Furthermore, the concentration range of quinidine, which inhibited voltage-gated K+ channel currents in electrophysiological assay, was consistent with that of quinidine inhibiting cell proliferation and inducing cell apoptosis. In U87-MG cells treated with quinidine (100 μmol/l), 11 of 2,042 human microRNAs (miRNAs) were upregulated and 16 were downregulated as detected with the miRNA array analysis. The upregulation of miR-149-3p and downregulation of miR-424-5p by quinidine treatment were further verified by using quantitative real-time PCR. In addition, using miRNA target prediction program, putative target genes related to cell proliferation and apoptosis for two differentially expressed miRNAs were predicted. Taken together, these data suggested that the anti-proliferative and pro-apoptosis effect of voltage-gated K+ channel blocker quinidine in human glioma cells was mediated at least partly through regulating expression of miRNAs, and provided further support for the mechanisms of voltage-gated K+ channels in mediating cell proliferation and apoptosis.

Introduction

Potassium channels (K+ channels) are the most diverse ion channels on the plasma membrane of mammalian cells (1). Accumulating evidence has proved that a variety of K+ channels, including voltage-gated (2), calcium-activated (3), two-pore domain (4) and inward rectifier (5) K+ channels are overexpressed in tumorous tissues compared to their healthy counterparts. They control the membrane potential as well as electrical signaling and are known to be involved in the regulation of proliferation, cell cycle progression and apoptosis of tumor cells (6).

Among all the K+ channels mentioned, most studies are directed at examining the impact of voltage-gated K+ channels on the proliferation of tumor cells (1). Voltage-gated K+ channel blockers, such as 4-aminopyridine, and tetraethylammonium, have been shown to inhibit cell proliferation and growth of tumor via an arrest in the G_0/G_1 transition during the cell cycle (7). Quinidine, another commonly used voltage-gated K+ channel blocker, can reduce the proliferation of tumor cells, such as human malignant mesothelioma cells and rat C6 glioma cells (8,9). However, the precise cellular mechanisms by which voltage-gated K+ channel activity contributes to cell proliferation and apoptosis are not clear yet.

MicroRNAs (miRNAs) are small non-coding RNAs that regulate gene expression through degradation of mRNA or translational inhibition of target mRNA (10). miRNAs act as key mediators in the progression and transformation of tumor through their regulation of proliferation, differentiation, and apoptosis (11). While many aspects of miRNA-induced protein regulation are known, there is a growing need to uncover the complex regulatory mechanisms governing the activation and suppression of miRNA expression (12). Interestingly, alterations in expression and function of ion channels/transporters have been shown to result in changes in expression of miRNAs (13). For example, some of the miRNAs, such as miR-155, -21, -27, -192 and -23, are regulated by cystic fibrosis transmem-

Correspondence to: Professor Chao-Ying Li, Wuhan Institutes of Biomedical Sciences, Jianghan University, Wuhan Economic and Technological Development Zone, Wuhan, Hubei 430056, P.R. China
E-mail: licy.whibs.corresp@outlook.com

brane conductance regulator, a cAMP-activated anion channel conducting both Cl^- and $HCO3^-$ (14). miR-21 and -30a, both of which are implicated in cancer development (15,16), are regulated by L-type Ca^{2+} channels (17). However, there is scarce literature on the effect of voltage-gated K^+ channels on miRNA expression.

In this study, we investigated the effect of quinidine on cell proliferation, apoptosis and expression of miRNAs of human glioma cell line U87-MG, and tried to find out whether quinidine affects cell proliferation and apoptosis by regulating miRNA expression. The results showed that the anti-proliferative and pro-apoptosis effect of quinidine in human glioma cells was mediated at least partly through regulating expression of miRNAs and provided further support for the mechanisms of voltage-gated K^+ channels in mediating cell proliferation and apoptosis.

Materials and methods

Reagents. Quinidine, 3-(4,5-dimethylthiazol-2-yl)-2,5-diphenyltetrazolium bromide (MTT) and tetrodotoxin (TTX) were products of the Sigma-Aldrich Corp. (St. Louis, MO, USA). RPMI-1640 medium and fetal bovine serum (FBS) were obtained from Life Technologies (Carlsbad, CA, USA). Annexin V-fuorescein isothiocyanate/propidium iodide (Annexin V-FITC/PI) apoptosis detection kit was procured from Wuhan Antgene Biotechnology Co.,Ltd. (Hubei, China). Caspase-3, -8 and -9 activity assay kits were obtained from Beyotime Institute of Biotechnology (Jiangsu, China). All other chemicals were of standard analytical grade.

Cell culture. Human glioma U87-MG cells were purchased from American Type Culture Collection (ATCC) (Manassas, VA, USA) and grown in RPMI-1640 supplemented with 10% FBS and 100 U penicillin/streptomycin in 5% CO_2 at 37˚C. Cells were passaged every three days and maintained at exponential growth to ~80% confluence for later experiments.

MTT cell proliferation assay. Briefly, cells were seeded at 5,000 cells/well into a 96-well plate and incubated overnight. After exposure to different concentrations of quinidine for 48 h, MTT solution (final concentration 0.5 mg/ml) was added to each well and the samples were incubated for another 4 h. Subsequently, the supernatant was removed and cells were dissolved in 150 μl DMSO. Finally, absorbance at 570 nm was measured by using a 96-well microplate reader (Thermo Fisher Scientific, Inc., Waltham, MA, USA).

Annexin V-FITC/PI apoptosis assay. Cells were double-stained by using an Annexin V-FITC/PI apoptosis detection kit. Briefly, cells were seeded at $5x10^6$ cells per flask into cultured flasks and incubated overnight. After exposure to different concentrations of quinidine for 48 h, cells were harvested and washed with cold PBS twice, and resuspended in Annexin V binding buffer. Then 5 μl of FITC-labeled Annexin V and 5 μl of PI were added. Cells were gently oscillated and incubated for 15 min at room temperature in the dark. After addition of 200 μl binding buffer to each tube, cells were analyzed on a flow cytometer (Becton-Dickinson, Franklin Lakes, NJ, USA) within 1 h.

Caspase activity assay. The activities of caspase-3, -8 and -9 were determined using the activity assay kits. To evaluate the activity of caspase, cell lysates were prepared after treatment with different concentrations of quinidine. Assays were performed on 96-well microtitre plates by incubating 10 μl protein of cell lysate per sample in 80 μl reaction buffer [1% NP-40, 20 mmol/l Tris-HCl (pH 7.5), 137 mmol/l Nad and 10% glycerol] containing 10 μl caspase substrate (Ac-DEVD-pNA for caspase-3, Ac-IETD-pNA for caspase-8, Ac-LEHD-pNA for caspase-9) (2 mmol/l). Lysates were incubated at 37˚C for 4 h. Samples were measured with a microplate reader at an absorbance of 405 nm. The detail analysis procedure is described in the manufacturer's protocol.

Electrophysiological assay. Membrane currents were recorded using a whole-cell voltage clamp and borosilicate glass pipettes (outer diameter, 1.5 mm; direct current resistance, 3-6 MΩ) constructed using a two-step puller (P-97; Sutter Instrument, Novato, CA, USA). To investigate the voltage-gated K^+ currents, the pipette solution consisted of 140 mmol/l KCl, 2.5 mmol/l $MgCl_2$, 10 mmol/l HEPES, 11 mmol/l EGTA and 5 mmol/l ATP, and the pH was adjusted to 7.2 (18). The cells were bathed in an extracellular solution containing 135 mmol/l NaCl, 5.4 mmol/l KCl, 1.0 mmol/l $MgCl_2$, 0.33 mmol/l NaH_2PO_4, 1.8 mmol/l $CaCl_2$, 10 mmol/l HEPES and 10 mmol/l D-glucose with 1 μmol/l TTX. The osmolarity was adjusted to 330 mosmol/l with sucrose, and the pH was adjusted to 7.4. Whole-cell patch clamp recordings were performed at room temperature using a patch clamp amplifier (Axon-200B; Axon Instruments, Union City, CA, USA) (19). Adjustments of capacitance and series resistance compensation were performed before the membrane currents were recorded. The membrane currents were filtered at 10 kHz (-3 dB), and the data were processed using Clampfit (Axon Instruments).

Microarray analysis of miRNAs gene expression. After treated with 100 μmol/l quinidine for 48 h, cells were harvested in PBS, collected by centrifugation, and total RNA extracted using the miRNeasy kit (Qiagen, Hilden, Germany) according to manufacturer's instructions. The experiment was repeated three times. Quantity and quality of RNA was determined by absorbance (260 and 280 nm). LC Sciences (Houston, TX, USA) performed microarray assay using 5 mg total RNA which was size fractioned using a YM-100 Micron centrifugal filter (Millipore, Billerica, MA, USA) and the small RNAs (<300 nt) isolated were 3'-extended with a poly(A) tail using poly(A) polymerase. Three biological samples of RNA were pooled and array was performed using quadruplicate internal repeats of pooled RNA as previously described (12). Data were analyzed by first subtracting the background and normalization of array was to statistical mean of all detectable transcripts. System related variation of data was corrected using LOWESS filter (locally-weighted regression) method (12). Probes were single channel and detected signals greater than background plus thre times the standard deviation was derived.

Quantitative real-time PCR for miRNA expression. To confirm the miRNA levels obtained from the microarray results, expression of miRNAs was assessed using quantitative real-time PCR. Total cellular RNA was extracted from each of

Table I. Sequences of the primer pairs used in quantitative real-time PCR.

miRNA	Reverse transcription (5'→3')	Forward (5'→3')	Reverse (5'→3')
miR-149-3p	CTATACCATAAGCGAGCAGTAGCGC GATGGTATAGGCACAGCC	TTGACGAGGGAG GGACGG	GCCATAAGCGAG CAGTAGCG
miR-25-3p	GTCGTATCCAGTGCAGGGTCCGAGG TATTCGCACTGGATACGACTCAGAC	CGCGGCATTGCAC TTGTCT	CAGTGCAGGGTCC GAGGTATTC
miR-100-5p	GTCGTATCCAGTGCAGGGTCCGAGG TATTCGCACTGGATACGACCACAAG	GCGAACCCGTAG ATCCGAA	CCAGTGCAGGGTC CGAGG
miR-424-5p	CTATACCATAAGCGAGCAGTAGCGC GATGGTATAGTTCAAAAC	CGGCGGCAGCAG CAAT	GCCATAAGCGAG CAGTAGCG
miR-365a-3p	GCGTGGTCCACACCACCTGAGCCGC CACGACCACGCATAAGGAT	GCCGCCTAATGCC CCTAA	TCCACACCACCTG AGCCG
RNU6B	GTCGTATCCAGTGCAGGGTCCGAGG TATTCGCACTGGATACGACAAAAAT	CAAATTCGTGAAG CGTTCCATA	AGTGCAGGGTCCG AGGTATTC

miRNA, microRNA.

the experimental groups using Qiagen miRNeasy RNA purification system according to the manufacturer's instructions. Quantity and quality of RNA was determined by absorbance (260 and 280 nm). Reverse transcription was performed using gene specific primers. The sequences of the primer pairs are shown in Table I. RNU6B was taken as an internal control. Quantitative real-time PCR was performed using Platinum SYBR-Green qPCR SuperMix-UDG (Invitrogen Life Technologies Carlsbad, CA, USA). The reactions were carried out in a 96-well optical plate at 95°C for 10 min and then amplified for 15 sec at 90°C, followed by 30 sec at 60°C for 40 cycles. The relative value of each miRNA was calculated using the $2^{-\Delta\Delta Ct}$ method, where Ct is the number of cycles at which the application reaches a threshold, as determined by SDS software v1.2 (Applied Biosystems, Inc., Foster City, CA, USA). Thermal denaturation was administered at the conclusion of the qPCR to determine the number of the products that were present in the reaction. Each reverse transcription and qPCR assay was performed in triplicate.

Bioinformatic analysis of miRNAs. Changes in expression of miRNAs between the control and quinidine-treated groups were selected and their putative cellular target genes were predicted using TargetScan (http://www.targetscan.org/). Using gene ontology (GO) (http://geneontology.org/) and Kyoto Encyclopedia of Genes and Genomes (KEGG) analysis tool (http://www.genome.jp/kegg/), the target genes were categorized into the following two groups: apoptosis and cell proliferation.

Statistical analysis. Data were expressed as mean ± standard error (mean ± SE). Statistical significance was assessed by using paired Student's t-test. $P < 0.05$ was considered to be statistically significant.

Results

Effect of quinidine on the proliferation of U87-MG cells. To measure the effect of quinidine on the proliferation of

U87-MG cells, cells were treated with various concentrations of quinidine (12.5, 25, 50, 100, 200, 400 and 800 μmol/l) for 48 h, and MTT assay was used to determine the number of the live cells remaining after the drug treatment. As shown in Fig. 1A, quinidine significantly inhibited the cell proliferation of U87-MG cells in a dose-dependent manner ($P < 0.01$). The value of IC_{50} was calculated to be 58.96 μmol/l at 48 h.

Effect of quinidine on the apoptosis of U87-MG cells. To determine whether the reduced cell viability by quinidine was related to apoptotic cell death, the effect of quinidine on apoptosis of U87-MG cells was studied by Annexin V-FITC/PI staining. As illustrated in Fig. 1B, quinidine increased the percentage of apoptotic cells in a concentration-dependent manner, and the apoptotic rates of U87-MG cells treated with 25, 50 and 100 μmol/l quinidine were 9.9, 29.6 and 53.1%, respectively. However, the effect of quinidine on necrosis was slight. At 100 μmol/l, quinidine only induced necrosis in ~2.5% of U87-MG cells, indicating that quinidine could induce apoptosis of U87-MG cells without causing obvious necrosis.

Apoptosis is always executed in a caspase-8-regulated plasma membrane extrinsic pathway and/or caspase-9-regulated mitochondrial intrinsic pathway (20). To determine whether caspases were activated by quinidine, we examined the activities of caspase-3, -8 and -9 in quinidine-treated U87-MG cells. As shown in Fig. 1C, quinidine treatment (25, 50 and 100 μmol/l) resulted in a dose-dependent activation of the initiator caspases-9, and the executor caspase-3. Additionally, activation of caspase-8 was also observed, but the activities of caspase-8 in quinidine-treated cells were not significantly different from that of control cells. These data implied that both mitochondrial and death receptor pathways were involved in the apoptotic process induced by quinidine in U87-MG cells, and the mitochondrial pathway was the main mode.

Effect of quinidine on K⁺ currents in U87-MG cells. To determine whether quinidine inhibited cell proliferation via
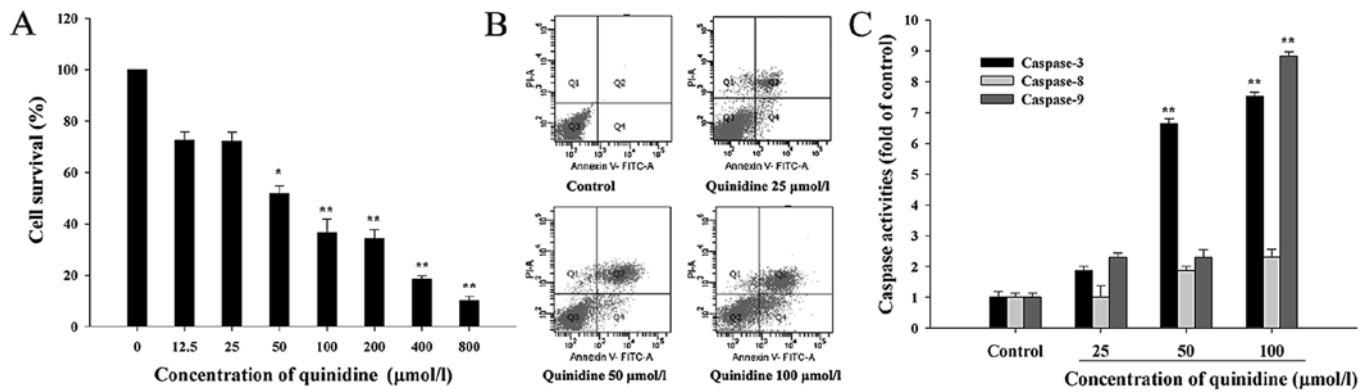
Figure 1. Effect of quinidine on cell proliferation and apoptosis in U87-MG cells. U87-MG cells were treated with the indicated concentrations of quinidine for 48 h. (A) Cell proliferation was suppressed in a dose-dependent manner. The suppression was significant in the range of 50-800 μmol/l of quinidine in U87-MG cells. (B) Quinidine-treated cells were labeled with both Annexin V-FITC and PI and subsequently assessed by flow cytometry. The results showed that quinidine could induce apoptosis in U87-MG cells in a dose-dependent manner, without causing obvious necrosis. (C) Caspase activity was determined with substrates appropriate for each caspase (caspase-3, Ac-DEVD-pNA; caspase-8, Ac-IETD-pNA; caspase-9, Ac-LEHD-pNA). The values represent mean ± SD. [*]P<0.05 and [**]P<0.01, compared to the group treated with a solvent control.
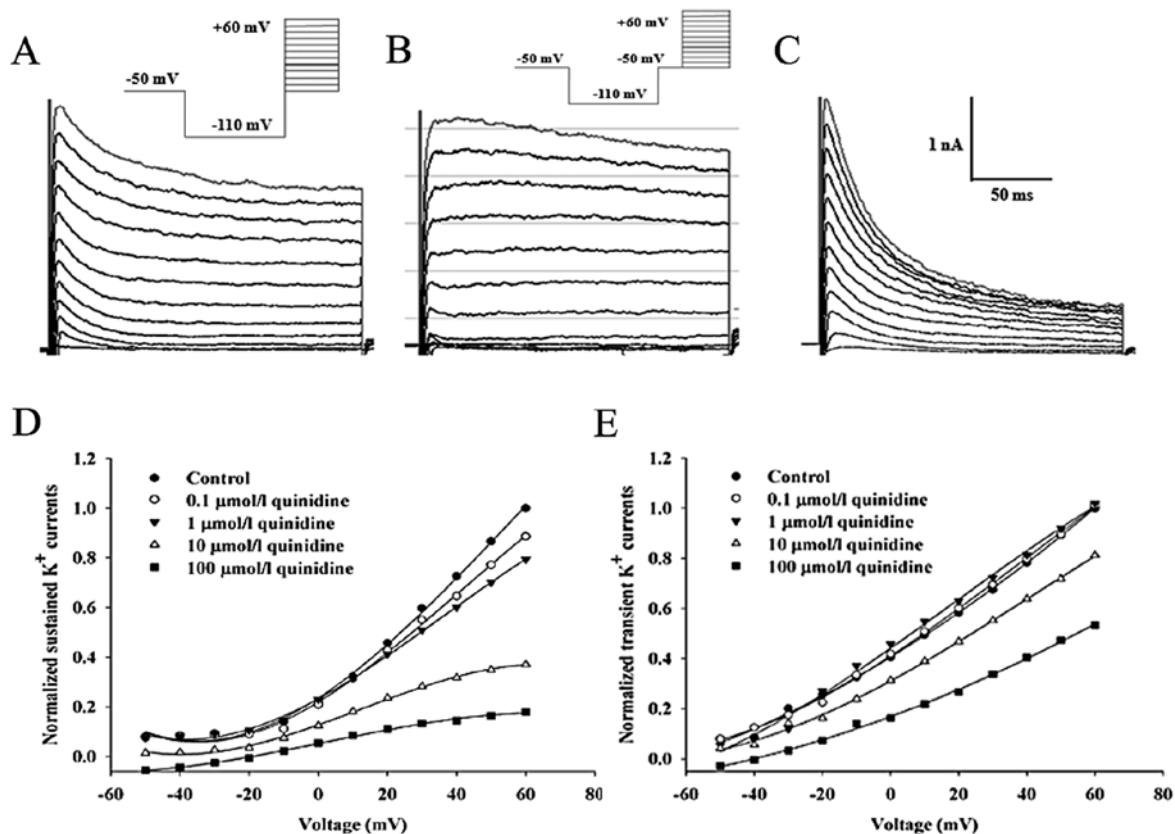

Figure 2. Effect of quinidine on K⁺ currents in U87-MG cells. (A) Representative traces of total voltage-gated K⁺ currents (bottom) evoked by voltage depolarizing step voltage protocol shown on the top. (B) The slow sustained K⁺ currents (bottom) recorded from the same cell evoked by depolarization protocol shown on the top. (C) The fast transient K⁺ currents were obtained by subtracting the sustained currents from the total voltage-gated K⁺ currents. (D) Quinidine suppressed current-voltage curve of sustained K⁺ currents. (E) Quinidine also suppressed current-voltage curve of transient K⁺ currents, and higher concentration of quinidine was required to have similar effect on transient K⁺ currents.

blockage of voltage-gated K⁺ currents (21), we next studied the dose-dependent effects of quinidine on voltage-gated K⁺ currents in U87-MG cells. The voltage-gated K⁺ currents consisted of two components (transient and sustained K⁺ currents) in U87-MG cells, and representative recordings of the voltage-gated K⁺ currents were evoked with a step-up depolarization protocol (Fig. 2). Briefly, the membrane potential was

pre-hyperpolarized from -50 to -110 mV for 100 msec, depolarized from -50 to +60 mV (10 mV increment per step, duration 200 msec), and subsequently restored to the original depolarizing potential of -50 mV (Fig. 2A). Depolarizing the voltage from -110 to -50 mV and maintaining the level of -50 mV for 100 msec inactivated transient K⁺ currents, and a further depolarization voltage step from -50 to +60 mV evoked sustained

Table II. Microarray analysis of miRNA expression in U87-MG cells treated with quinidine.

miRNA	Fold	P-value	Localization	Up-, down-regulation
hsa-miR-1234-5p	1.36±0.06	0.004	chr8: 145625476-145625559 (-)	Up
hsa-miR-4497	2.64±0.21	0.013	chr12: 110271153-110271241 (+)	Up
hsa-miR-4707-5p	1.65±0.26	0.022	chr14: 23426159-23426238 (-)	Up
hsa-miR-149-3p	2.00±0.15	0.023	chr2: 241395418-241395506 (+)	Up
hsa-miR-3196	1.64±0.06	0.008	chr20: 61870131-61870194 (+)	Up
hsa-miR-762	1.47±0.06	0.035	chr16: 30905224-30905306 (+)	Up
hsa-miR-4655-5p	3.22±0.42	0.037	chr7: 883816-1883889 (-)	Up
hsa-miR-4530	1.81±0.36	0.046	chr19: 39900263-39900318 (-)	Up
hsa-miR-2392	2.14±0.60	0.047	chr14: 101280828-101280911 (+)	Up
hsa-miR-4646-5p	2.01±0.19	0.049	chr6: 31668806-31668868 (-)	Up
hsa-miR-204-3p	2.28±0.57	0.049	chr9: 73424891-73425000 (-)	Up
hsa-let-7a-5p	0.79±0.02	0.012	chr9: 96938239-96938318 (+)	Down
hsa-miR-25-3p	0.58±0.02	0.014	chr7: 99691183-99691266 (-)	Down
hsa-let-7i-5p	0.76±0.03	0.016	chr12: 62997466-62997549 (+)	Down
hsa-let-7d-5p	0.75±0.03	0.020	chr9: 96941116-96941202 (+)	Down
hsa-miR-100-5p	0.60±0.05	0.037	chr11: 122022937-122023016 (-)	Down
hsa-miR-10b-5p	0.63±0.12	0.032	chr2: 177015031-177015140 (+)	Down
hsa-miR-9-5p	0.80±0.07	0.036	chr1: 156390133-156390221 (-)	Down
hsa-miR-5100	0.68±0.01	0.038	chr10: 43493011-43493129 (+)	Down
hsa-miR-27a-3p	0.81±0.04	0.038	chr19: 13947254-13947331 (-)	Down
hsa-miR-29b-3p	0.76±0.09	0.048	chr7: 130562218-130562298 (-)	Down
hsa-let-7b-5p	0.68±0.06	0.048	chr22: 46509566-46509648 (+)	Down
hsa-miR-424-5p	0.51±0.02	0.002	chrX: 133680644-133680741 (-)	Down
hsa-miR-365a-3p	0.55±0.06	0.024	chr16: 14403142-14403228 (+)	Down
hsa-miR-450a-5p	0.69±0.06	0.025	chrX: 133674371-133674461 (-)	Down
hsa-let-7d-3p	0.73±0.04	0.029	chr9: 96941116-96941202 (+)	Down
hsa-miR-495-5p	0.16±0.06	0.031	chr14: 101500092-101500173 (+)	Down

The results presented fold change of signal ratio of 100 μmol/l quinidine-treated cells to untreated control cells. The raw data were normalized and analyzed with software of MatLab version 7.4, which produced an average value of the three spot replications of each miRNA. Chromosome localization of miRNAs as refered in miRBase sequences (http://microrna.sanger.ac.uk). miRNA, microRNA.

K^+ currents (Fig. 2B). The transient component (Fig. 2C) was then visualized in isolation using point-by-point subtraction of the sustained component (Fig. 2B) from the total outward current (Fig. 2A). As illustrated in Fig. 2D and E, quinidine shifted the current-voltage curves of transient and sustained K^+ currents downward at different depolarization potentials in a dose-dependent manner. Quinidine was more potent in suppressing sustained than transient K^+ currents. For instance, at the depolarizing voltage of +60 mV, the percentage inhibition by 100 μmol/l quinidine of transient and sustained K^+ currents were ~46.64 and 82.04%, respectively (Fig. 2D and E).

Effect of quinidine on miRNA expression in U87-MG cells. To examine the miRNAs involved in quinidine-induced cytotoxicity, total RNA was extracted from U87-MG cells treated with 100 μmol/l quinidine for 48 h. The μParaflo® miRNA microarray containing 2,042 mature human miRNA probes was used to identify the cellular miRNA expression profiles. We found that the expression of specifc miRNAs in quinidine-treated U87-MG cells was signifcantly altered when compared to that in untreated (control) cells. The results of quinidine-regulated miRNAs and their chromosomal locations are summarized in Table II. Of the 2,042 human miRNAs tested, 11 miRNAs were upregulated and 16 miRNAs were downregulated in our experiment.

Based on previous published reports (22,23), we selected the following five miRNAs: the upregulated miR-149-3p, the downregulated miR-25-3p, miR-100-5p, miR-424-5p and miR-365a-3p and measured their expression levels by quantitative real-time PCR. After individual miRNA level in each sample was quantified and normalized to U6 expression, quantitative PCR data confirmed that the expressions of miR-149-3p and miR-424-5p were up- and downregulated significantly in the quinidine-treated U87-MG cells, respectively (P<0.05). Although the expressions of miR-25-3p, miR-100-5p and miR-365a-3p were downregulated in microarray analysis, there were no statistically significant differences by real-time PCR analysis (Fig. 3).
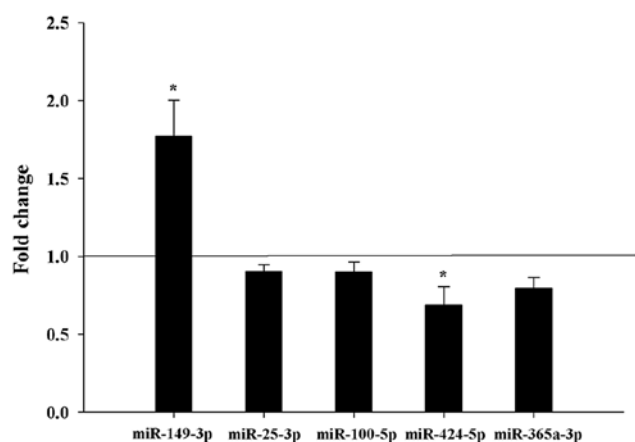
Figure 3. Validation of microRNAs (miRNAs) expression by quantitative real-time PCR. The cells were treated with 100 μmol/l quinidine for 48 h. The expressions of upregulated miR-149-3p, as well as the downregulated miR-25-3p, miR-100-5p, miR-424-5p and miR-365a-3p in U87-MG cells were verified. The results of quantitative real-time PCR presented fold change of miRNA expression in 100 μmol/l quinidine-treated cells to untreated control cells. The results for the five selected miRNAs were consistent with the miRNA array results, and the expression of miR-149-3p and miR-424-5p were up- and downregulated significantly in the quinidine-treated U87-MG cells, respectively (P<0.05). Fold change of miRNA expression is presented in $2^{-\Delta\Delta Ct}$. *P<0.05, compared to the group treated with a solvent control.
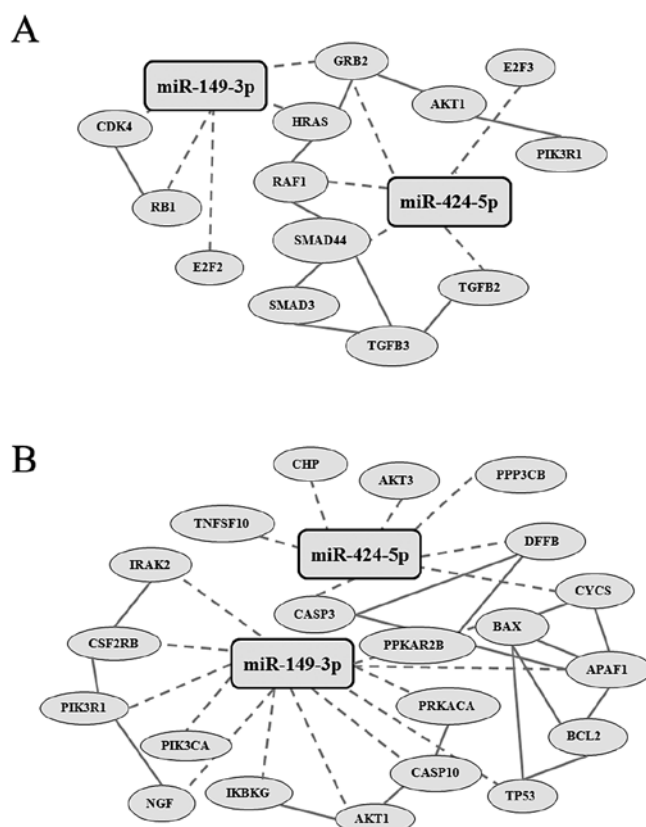

Figure 4. Network of differentially expressed microRNAs (miRNAs) and their putative targets. In the network, miRNAs are represented by rectangle shapes and targets are represented by oval shapes. Solid lines show target-target interactions, and dashed lines show miRNA-target interactions.

Prediction of potential targets for verified miRNAs. Since the cellular functions of miRNAs are directly mediated by controlling their target gene expression, we further analyzed the putative target genes of the miRNAs and the functional relationship between the gene and anticancer properties using bioinformatic tools. First, the miRBase target database tool, MicroCosm, revealed that 3,803 genes were potentially targeted by quinidine-specific miRNAs. Moreover, since quinidine promotes the death of cancer cells through its anti-proliferative and pro-apoptotic activities, we selected genes with functions related to cell proliferation and apoptosis by using the GO and KEGG analysis tool. Consistent with the previous finding, the GO and KEGG analysis results showed that several target genes of the quinidine-responsive miRNAs were functionally involved in anticancer pathways. These sets of genes are shown in Fig. 4.

Discussion

Since the pioneering study in lymphocytes by DeCoursey *et al* in 1984 (24), accumulating evidence has indicated that K+ channels are relevant players in controlling cell proliferation and apoptosis of various tumor cells. Of all K+ channels, most studies are devoted to the impact of voltage-gated K+ channels on proliferation and apoptosis of tumor cells (6,25). Gliomas are the most common malignant brain tumors (26), the levels of expression of Kv1.5 and 1.3 channel subtypes discriminated between various glioma groups, and a clear differential expression of Kv1.5 was observed according to malignancy grade (27). We have shown previously that voltage-gated K+ channels play roles in controlling cell proliferation and apoptosis of glioma cells (7). However, the underlying mechanisms remain poorly understood.

It was reported that voltage-gated K+ channel blocker quinidine can inhibit the proliferation of human malignant mesothelioma cells and rat C6 glioma cells (8,9). However, the effects of quinidine on cell proliferation of human glioma cells and apoptosis of tumor cells have not been studied yet. In the present investigation, we found that quinidine could inhibit cell proliferation of human glioma U87-MG cells in a dose-dependent manner. The increased apoptosis rate was also observed after incubation of the cells with certain concentration of quinidine, and the cells displayed typical apoptotic features, including chromatin condensation, indicating that quinidine could induce apoptosis in U87-MG cells without causing conspicuous necrosis.

Apoptosis was determined as activation of crucial caspases, such as initiator caspase-9 of intrinsic apoptosis pathway, initiator caspase-8 of extrinsic death receptor pathway and executioner caspase-3 (28). We investigated whether one or both the caspase cascades were activated in quinidine-induced cell apoptosis, and found that caspase-9 activation was remarkably triggered in 100 μmol/l quinidine-treated cells through the mitochondria initiated caspase activation cascade.

Previous reports showed that pharmacological blockades of voltage-gated K+ channels lead to cell proliferation inhibition (29). Fraser *et al* have reported that the IC_{50} value of 4-aminopyridine in blocking voltage-gated K+ channel currents of rat prostate cancer AT-2 cells was 4±2 mmol/l (30), which was close to the IC_{50} value of 4-aminopyridine in inhibiting cell proliferation of human glioma U87-MG cells (7). Our

electrophysiological and pharmacological results proved that quinidine inhibited cell proliferation and apoptosis in the concentration range required to block voltage-gated K⁺ channel currents, indicating that quinidine potentially inhibited cell proliferation and induced apoptosis by blocking voltage-gated K⁺ channel activities. These data provided further support for the roles of voltage-gated K⁺ channels in mediating cell proliferation and apoptosis.

Many miRNAs have been reported to have an oncogenic or a tumor suppressor function and to be involved in tumor cell proliferation and apoptosis. However, little is known about the relationship between miRNA expression and voltage-gated K⁺ channels of tumor cells. The present study demonstrated that quinidine significantly altered expression of miRNAs in U87-MG cells, including 11 upregulated and 16 downregulated miRNAs. Among the miRNAs regulated by quinidine, some have been reported to be tumor suppressors. For instance, miR-149 and -204 function as tumor suppressors and trigger growth inhibition in human glioma cells (23,31). In addition, some miRNAs have been reported to be oncogenic. For instance, knockdown or reduction of miR-10b led to glioma cell apoptosis, cell growth inhibition, and suppressed tumorigenicity (32).

miR-149 is considered to be a potential tumor suppressor. Suppression of miR-149 has been demonstrated in various human cancers, such as colorectal cancer (33) and HeLa cells (34). A recent miRNA microarray study has shown that miR-149 was downregulated significantly in grade I-IV astrocytomas, and overexpression of miR-149 inhibited glioblastoma cell proliferation and migration (35). miR-424 is considered to be a potential oncogenic miRNA. It is significantly upregulated and involved in proliferation, migration and invasion, and chemoresistant in different human cancers (23,36,37). Noteworthy, there are no reports regarding the role of miR-424 in glioma cells. In the current study, we verified that miR-149-3p was upregulated in 100 μmol/l quinidine-treated cells by quantitative real-time PCR, whereas miR-424-5p was downregulated. This is the first report to indicate that the blockade of voltage-gated K⁺ channels could affect the expression of miR-149-3p/miR-424-5p in tumor cells. The GO and KEGG analysis results showed that the predicted target genes of miR-149-3p and miR-424-5p were functionally involved in cell proliferation and apoptosis process. Future studies are needed to investigate the molecular mechanism of miR-149-3p and miR-424-5p in quinidine-induced anticancer effect.

In conclusion, the present study shows that voltage-gated K⁺ channel blocker quinidine inhibits proliferation and induces apoptosis of U87-MG glioma cells in a dose-dependent manner. A subset of human miRNAs reveals significant changes in expression in response to quinidine in the U87-MG cell line. These results suggest that the antitumor effect of voltage-gated K⁺ channel blocker quinidine in human glioma cells was mediated at least partly through regulating miRNA expression, and provide new insight into the understanding of the molecular mechanisms of voltage-gated K⁺ channels in mediating cell proliferation and apoptosis.

Acknowledgements

References

1. Pardo LA: Voltage-gated potassium channels in cell proliferation. Physiology (Bethesda) 19: 285-292, 2004.
2. Kunzelmann K: Ion channels and cancer. J Membr Biol 205: 159-173, 2005.
3. Abdullaev IF, Rudkouskaya A, Mongin AA and Kuo Y-H: Calcium-activated potassium channels BK and IK1 are functionally expressed in human gliomas but do not regulate cell proliferation. PLoS One 5: e12304, 2010.
4. Mu D, Chen L, Zhang X, See LH, Koch CM, Yen C, Tong JJ, Spiegel L, Nguyen KC, Servoss A, Peng Y, Pei L, Marks JR, Lowe S, Hoey T, Jan LY, McCombie WR, Wigler MH and Powers S: Genomic amplification and oncogenic properties of the KCNK9 potassium channel gene. Cancer Cell 3: 297-302, 2003.
5. Huang L, Li B, Li W, Guo H and Zou F: ATP-sensitive potassium channels control glioma cells proliferation by regulating ERK activity. Carcinogenesis 30: 737-744, 2009.
6. Fiske JL, Fomin VP, Brown ML, Duncan RL and Sikes RA: Voltage-sensitive ion channels and cancer. Cancer Metastasis Rev 25: 493-500, 2006.
7. Ru Q, Tian X, Wu YX, Wu RH, Pi MS and Li CY: Voltage-gated and ATP-sensitive K⁺ channels are associated with cell proliferation and tumorigenesis of human glioma. Oncol Rep 31: 842-848, 2014.
8. Utermark T, Alekov A, Lerche H, Abramowski V, Giovannini M and Hanemann CO: Quinidine impairs proliferation of neurofibromatosis type 2-deficient human malignant mesothelioma cells. Cancer 97: 1955-1962, 2003.
9. Weiger TM, Colombatto S, Kainz V, Heidegger W, Grillo MA and Hermann A: Potassium channel blockers quinidine and caesium halt cell proliferation in C6 glioma cells via a polyamine-dependent mechanism. Biochem Soc Trans 35: 391-395, 2007.
10. Bushati N and Cohen SM: microRNA functions. Annu Rev Cell Dev Biol 23: 175-205, 2007.
11. Visone R and Croce CM: MiRNAs and cancer. Am J Pathol 174: 1131-1138, 2009.
12. Martin EC, Bratton MR, Zhu Y, Rhodes LV, Tilghman SL, Collins-Burow BM and Burow ME: Insulin-like growth factor-1 signaling regulates miRNA expression in MCF-7 breast cancer cell line. PLoS One 7: e49067, 2012.
13. Jiang X, Zhang JT and Chan HC: Ion channels/transporters as epigenetic regulators? - a microRNA perspective. Sci China Life Sci 55: 753-760, 2012.
14. Bhattacharyya S, Balakathiresan NS, Dalgard C, Gutti U, Armistead D, Jozwik C, Srivastava M, Pollard HB and Biswas R: Elevated miR-155 promotes inflammation in cystic fibrosis by driving hyperexpression of interleukin-8. J Biol Chem 286: 11604-11615, 2011.
15. Gao W, Lu X, Liu L, Xu J, Feng D and Shu Y: MiRNA-21: a biomarker predictive for platinum-based adjuvant chemotherapy response in patients with non-small cell lung cancer. Cancer Biol Ther 13: 330-340, 2012.
16. Kumarswamy R, Volkmann I and Thum T: Regulation and function of miRNA-21 in health and disease. RNA Biol 8: 706-713, 2011.
17. Carrillo ED, Escobar Y, González G, Hernández A, Galindo JM, García MC and Sánchez JA: Posttranscriptional regulation of the β2-subunit of cardiac L-type Ca²⁺ channels by MicroRNAs during long-term exposure to isoproterenol in rats. J Cardiovasc Pharmacol 58: 470-478, 2011.
18. Akamine T, Nishimura Y, Ito K, Uji Y and Yamamoto T: Effects of haloperidol on K(+) currents in acutely isolated rat retinal ganglion cells. Invest Ophthalmol Vis Sci 43: 1257-1261, 2002.
19. Liu YW and Li CY: Inhibition of N-methyl-D-aspartate-activated current by bis(7)-tacrine in HEK-293 cells expressing NR1/NR2A or NR1/NR2B receptors. J Huazhong Univ Sci Technolog Med Sci 32: 793-797, 2012.
20. Bao Q and Shi Y: Apoptosome: a platform for the activation of initiator caspases. Cell Death Differ 14: 56-65, 2007.
21. Fishman MC and Spector I: Potassium current suppression by quinidine reveals additional calcium currents in neuroblastoma cells. Proc Natl Acad Sci USA 78: 5245-5249, 1981.

22. Pan SJ, Zhan SK, Pei BG, Sun QF, Bian LG and Sun BM: MicroRNA-149 inhibits proliferation and invasion of glioma cells via blockade of AKT1 signaling. Int J Immunopathol Pharmacol 25: 871-881, 2012.
23. Wu K, Hu G, He X, Zhou P, Li J, He B and Sun W: MicroRNA-424-5p suppresses the expression of SOCS6 in pancreatic cancer. Pathol Oncol Res 19: 739-748, 2013.
24. DeCoursey TE, Chandy KG, Gupta S and Cahalan MD: Voltage-gated K⁺ channels in human T lymphocytes: a role in mitogenesis? Nature 307: 465-468, 1984.
25. Jang SH, Kang KS, Ryu PD and Lee SY: Kv1.3 voltage-gated K(+) channel subunit as a potential diagnostic marker and therapeutic target for breast cancer. BMB Rep 42: 535-539, 2009.
26. Ru Q, Shang BY, Miao QF, Li L, Wu SY, Gao RJ and Zhen YS: A cell penetrating peptide-integrated and enediyne-energized fusion protein shows potent antitumor activity. Eur J Pharm Sci 47: 781-789, 2012.
27. Preussat K, Beetz C, Schrey M, Kraft R, Wölfl S, Kalff R and Patt S: Expression of voltage-gated potassium channels Kv1.3 and Kv1.5 in human gliomas. Neurosci Lett 346: 33-36, 2003.
28. Mutlu A, Gyulkhandanyan AV, Freedman J and Leytin V: Activation of caspases-9, -3 and -8 in human platelets triggered by BH3-only mimetic ABT-737 and calcium ionophore A23187: caspase-8 is activated via bypass of the death receptors. Br J Haematol 159: 565-571, 2012.
29. Le Guennec JY, Ouadid-Ahidouch H, Soriani O, Besson P, Ahidouch A and Vandier C: Voltage-gated ion channels, new targets in anti-cancer research. Recent Pat Anticancer Drug Discov 2: 189-202, 2007.
30. Fraser SP, Grimes JA, Diss JK, Stewart D, Dolly JO and Djamgoz MB: Predominant expression of Kv1.3 voltage-gated K⁺ channel subunit in rat prostate cancer cell lines: electrophysiological, pharmacological and molecular characterisation. Pflugers Arch 446: 559-571, 2003.
31. Ying Z, Li Y, Wu J, Zhu X, Yang Y, Tian H, Li W, Hu B, Cheng SY and Li M: Loss of miR-204 expression enhances glioma migration and stem cell-like phenotype. Cancer Res 73: 990-999, 2013.
32. Gabriely G, Yi M, Narayan RS, Niers JM, Wurdinger T, Imitola J, Ligon KL, Kesari S, Esau C, Stephens RM, Tannous BA and Krichevsky AM: Human glioma growth is controlled by microRNA-10b. Cancer Res 71: 3563-3572, 2011.
33. Wang F, Ma YL, Zhang P, Shen TY, Shi CZ, Yang YZ, Moyer MP, Zhang HZ, Chen HQ, Liang Y and Qin HL: SP1 mediates the link between methylation of the tumour suppressor miR-149 and outcome in colorectal cancer. J Pathol 229: 12-24, 2013.
34. Lin RJ, Lin YC and Yu AL: miR-149* induces apoptosis by inhibiting Akt1 and E2F1 in human cancer cells. Mol Carcinog 49: 719-727, 2010.
35. Li D, Chen P, Li XY, Zhang LY, Xiong W, Zhou M, Xiao L, Zeng F, Li XL, Wu MH and Li GY: Grade-specific expression profiles of miRNAs/mRNAs and docking study in human grade I-III astrocytomas. OMICS 15: 673-682, 2011.
36. Park YT, Jeong JY, Lee MJ, Kim KI, Kim TH, Kwon YD, Lee C, Kim OJ and An HJ: MicroRNAs overexpressed in ovarian ALDH1-positive cells are associated with chemoresistance. J Ovarian Res 6: 18, 2013.
37. Sand M, Skrygan M, Georgas D, Sand D, Hahn SA, Gambichler T, Altmeyer P and Bechara FG: Microarray analysis of microRNA expression in cutaneous squamous cell carcinoma. J Dermatol Sci 68: 119-126, 2012.